

Bifurcation diagrams in a class of Kolmogorov systems

G. Moza, C. Lazureanu*, F. Munteanu, C. Sterbeti, A. Florea†

Abstract

We study a two-dimensional Kolmogorov system when its two parameters vary in a small neighbourhood of the value 0. The local behavior of the system is described in terms of bifurcation diagrams.

1 Introduction

We consider in this work the following Kolmogorov class of systems

$$\begin{aligned} \frac{dx}{dt} &= 2x (\mu_1 + p_{11}x + p_{12}y + p_{13}xy + s_1x^2) \\ \frac{dy}{dt} &= 2y (\mu_2 + p_{21}x + p_{22}y + p_{23}x^2 + s_2y^2) \end{aligned}, \quad (1)$$

where $\mu = (\mu_1, \mu_2) \in \mathbb{R}^2$, $p_{ij} = p_{ij}(\mu)$ and $s_i = s_i(\mu)$ are smooth functions of their arguments, $i = 1, 2$, $j = 1, 2, 3$, $|\mu| = \sqrt{\mu_1^2 + \mu_2^2}$ is sufficiently small, $0 \leq |\mu| \ll 1$, and $p_{12}(0)p_{22}(0) \neq 0$. More difficult is the case $p_{12}(0)p_{22}(0) = 0$, which will be tackled in another work.

In general, differential systems of the form

$$\dot{x}_i = x_i \cdot P_i(x_1, \dots, x_n), \quad (2)$$

$i = 1, \dots, n$, $x_i = x_i(t)$, P_i smooth functions, are called Kolmogorov systems [8]. Their applications can be found in many areas, such as biology [2], [11], fluid dynamics (turbulence) [4] and plasma physics [7]. For example, a Kolmogorov three-dimensional system has been recently studied in [1] as a model for parasites dynamics. If P_i are polynomials, then (2) is a Lotka–Volterra system which is widely used in modeling interacting species of predator-prey type arising, for example, in biology [3], [5] and ecology [6], [9], [12].

Since many of these applications use positive variables, we will study the system (1) only in the first quadrant $Q1$, that is, when $x \geq 0$ and $y \geq 0$. However, a similar study can be performed for the other quadrants. It is worth mentioning that the axes $x = 0$ and $y = 0$ are invariant manifolds with respect to system's flow, thus, an orbit starting in the first quadrant cannot cross any of the two axes and travel in other quadrants. It remains forever (for all t where it is defined) in the first quadrant. This aspect is important in applications because, if a model of type (2) has practical relevance only when its variables x_i are positive (and this is the case in most of the models of this type), then, an orbit starting in the zone of practical relevance will never leave this zone to enter a zone which does not present interest, characterized by $x_i(t) < 0$ for some $i \in \{1, \dots, n\}$ and $t \in \mathbb{R}$. In other words, if the

*Department of Mathematics, Politehnica University of Timisoara, Romania; gheorghe.moza@upt.ro

†Department of Applied Mathematics, University of Craiova, Romania

starting state of a model lies in a zone of practical relevance, then the evolution of that state remains in the same zone for any time.

The paper is organized as it follows. After the introduction, in section 2 we present the main analytical results which describe the behavior of the system. In section 3 we present the bifurcation diagrams arising in the system. An in-depth study of the system is performed in this section, by finding the curves which separate a node from a focus. Such curves are in general ignored in typical bifurcation analysis but they are highly appreciated in practical models used in biology and engineering, for example. Differentiating between a node and a focus, twenty six different phase portraits are obtained in the bifurcation diagrams. Conclusive remarks end the article.

2 Analytical properties of the system

Depending on the signs of $p_{12}(0)$ and $p_{22}(0)$, the system leads to two different forms, one corresponding to 1) $p_{12}(0)p_{22}(0) < 0$ and the other to 2) $p_{12}(0)p_{22}(0) > 0$.

Indeed, let us consider first 1) with $p_{12}(0) < 0$ and $p_{22}(0) > 0$. Define the changes

$$\xi_1 = -p_{12}(\mu)x, \xi_2 = p_{22}(\mu)y \text{ and } t = 2\tau. \quad (3)$$

The transformation of variables $(x, y) \mapsto (\xi_1, \xi_2)$ is well defined for all $|\mu|$ small enough and is nonsingular because $p_{12}(0)p_{22}(0) \neq 0$.

It follows from (3) that the system (1) is locally topologically equivalent near the origin to

$$\begin{cases} \frac{d\xi_1}{dt} &= \xi_1 (\mu_1 - \theta(\mu)\xi_1 + \gamma(\mu)\xi_2 - M(\mu)\xi_1\xi_2 + N(\mu)\xi_1^2) \\ \frac{d\xi_2}{dt} &= \xi_2 (\mu_2 - \delta(\mu)\xi_1 + \xi_2 + S(\mu)\xi_1^2 + P(\mu)\xi_2^2) \end{cases}, \quad (4)$$

where the coefficients $\theta(\mu) = \frac{p_{11}(\mu)}{p_{12}(\mu)}$, $\gamma(\mu) = \frac{p_{12}(\mu)}{p_{22}(\mu)}$, $M(\mu) = \frac{p_{13}(\mu)}{p_{12}(\mu)p_{22}(\mu)}$, $N(\mu) = \frac{s_1(\mu)}{p_{12}^2(\mu)}$, $\delta(\mu) = \frac{p_{21}(\mu)}{p_{12}(\mu)}$, $S(\mu) = \frac{p_{23}(\mu)}{p_{12}^2(\mu)}$ and $P(\mu) = \frac{s_2(\mu)}{p_{22}^2(\mu)}$ are smooth functions in μ . In what follows, these coefficients are needed only at $\mu = 0$. In order to save symbols, we denote by $\theta(0) = \theta$, $\gamma(0) = \gamma$, $\delta(0) = \delta$, $N = N(0)$ and so on. Notice that $\theta = \frac{p_{11}(0)}{p_{12}(0)}$, $\gamma = \frac{p_{12}(0)}{p_{22}(0)}$ and $\delta = \frac{p_{21}(0)}{p_{12}(0)}$ are well-defined from $p_{12}(0)p_{22}(0) \neq 0$. Moreover, $\gamma < 0$ while $\theta\delta$ can be 0.

Remark 2.1. If $p_{12}(0) > 0$ and $p_{22}(0) < 0$, using the changes $\xi_1 = p_{12}(\mu)x$, $\xi_2 = -p_{22}(\mu)y$ and $t = -2\tau$, the system (1) reads

$$\begin{cases} \frac{d\xi_1}{dt} &= \xi_1 (-\mu_1 - \theta(\mu)\xi_1 + \gamma(\mu)\xi_2 + M(\mu)\xi_1\xi_2 - N(\mu)\xi_1^2) \\ \frac{d\xi_2}{dt} &= \xi_2 (-\mu_2 - \delta(\mu)\xi_1 + \xi_2 - S(\mu)\xi_1^2 - P(\mu)\xi_2^2) \end{cases},$$

which is of the same form as (4) if one denotes by $\tilde{\mu}_{1,2} = -\mu_{1,2}$, $\tilde{M}(\mu) = -M(\mu)$, $\tilde{N}(\mu) = -N(\mu)$, $\tilde{S}(\mu) = -S(\mu)$ and $\tilde{P}(\mu) = -P(\mu)$.

In the case 2), assume first $p_{12}(0) > 0$ and $p_{22}(0) > 0$. Then (1) is locally topologically equivalent near the origin to

$$\begin{cases} \frac{d\xi_1}{dt} &= \xi_1 (\mu_1 + \theta(\mu)\xi_1 + \gamma(\mu)\xi_2 + M(\mu)\xi_1\xi_2 + N(\mu)\xi_1^2) \\ \frac{d\xi_2}{dt} &= \xi_2 (\mu_2 + \delta(\mu)\xi_1 + \xi_2 + S(\mu)\xi_1^2 + P(\mu)\xi_2^2) \end{cases}, \quad (5)$$

by using the changes $\xi_1 = p_{12}(\mu)x$, $\xi_2 = p_{22}(\mu)y$ and $t = 2\tau$. We notice also that, the case $p_{12}(0) < 0$ and $p_{22}(0) < 0$ reduces to (5) by changes $\xi_1 = -p_{12}(\mu)x$, $\xi_2 = -p_{22}(\mu)y$ and $t = -2\tau$, using also new parameters such as $\tilde{\mu}_{1,2} = -\mu_{1,2}$ and renaming the coefficients M , N , S and P as needed.

Remark 2.2. *Since $\gamma(0) > 0$ in (5) and $\gamma(0) < 0$ in (4), the two systems are not necessarily locally topologically equivalent near the origin, thus, they should be studied separately. In this work we tackle the first case, $p_{12}(0)p_{22}(0) < 0$.*

Remark 2.3. *The axes $\xi_1 = 0$ and $\xi_2 = 0$ in (4) are invariant with respect to the system's flow and, by (3), $\xi_1 \geq 0$ and $\xi_2 \geq 0$ whenever $x \geq 0$ and $y \geq 0$. It follows that, the first quadrant of (1) is transformed by (3) in the first quadrant of (4), denoted by $Q1$. Thus, the new system (4) will be studied only in the first quadrant also.*

We approach in this work the first case, $p_{12}(0)p_{22}(0) < 0$, and more precisely the system (4) with $\theta(0)\delta(0) \neq 0$ and $\gamma(0) < 0$.

The first three equilibria of (4) are $O(0,0)$, $E_1(\xi_1, 0)$ and $E_2(0, \xi_2)$, where $\mu_1 - \theta\xi_1 + N\xi_1^2 = 0$ and $\mu_2 + \xi_2 + P\xi_2^2 = 0$, which, in their lowest terms become $\xi_1 = \frac{1}{\theta}\mu_1 + O(\mu_1^2)$ and $\xi_2 = -\mu_2 + O(\mu_2^2)$, for all $|\mu|$ sufficiently small.

The existence of a fourth equilibrium $E_3(\xi_1, \xi_2)$ is ensured by the Implicit Function Theorem (IFT) applied to the algebraic system

$$\mu_1 - \theta\xi_1 + \gamma\xi_2 - M\xi_1\xi_2 + N\xi_1^2 = 0 \text{ and } \mu_2 - \delta\xi_1 + \xi_2 + S\xi_1^2 + P\xi_2^2 = 0, \quad (6)$$

provided that

$$\theta - \gamma\delta \neq 0. \quad (7)$$

The coordinates of $E_3(\xi_1, \xi_2)$ are of the form

$$\xi_1 = \frac{\mu_1}{\theta - \gamma\delta} (1 + O(|\mu|)) - \frac{\gamma\mu_2}{\theta - \gamma\delta} (1 + O(|\mu|)) \text{ and } \xi_2 = \frac{\delta\mu_1}{\theta - \gamma\delta} (1 + O(|\mu|)) - \frac{\theta\mu_2}{\theta - \gamma\delta} (1 + O(|\mu|)). \quad (8)$$

We denote by $O(|\mu|^k) = \sum_{i+j \geq k} c_{ij}\mu_1^i\mu_2^j$ a Taylor series starting with terms of order at least $k \geq 1$.

Remark 2.4. *We are concerned in this work with local properties of the system (4) around the equilibrium points O , $E_{1,2}$ and E_3 when (μ_1, μ_2) moves in the parametric plane with $|\mu| = \sqrt{\mu_1^2 + \mu_2^2}$ sufficiently small.*

We state first the following result, which will be needed for studying the existence of bifurcation curves. Denote by $D \subset \mathbb{R}^2$ an open disc of center $(0,0)$ and radius $\varepsilon > 0$ sufficiently small, i.e. $D = \{(x, y), x^2 + y^2 < \varepsilon\}$ is a small neighborhood of $(0,0)$.

Lemma 2.5. *Let $F, G : D \subset \mathbb{R}^2 \rightarrow \mathbb{R}$ be two smooth functions of the form*

$$a) F(\mu_1, \mu_2) = a\mu_2(1 + O(|\mu|)) + b\mu_1(1 + O(|\mu|)), \text{ } ab \neq 0, \text{ and}$$

$$b) G(\mu_1, \mu_2) = a\mu_2^2(1 + O(|\mu|)) - 2b\mu_1\mu_2(1 + O(|\mu|)) + c\mu_1^2(1 + O(|\mu|)), \text{ } ac \neq 0. \text{ Then, when } |\mu|$$

is sufficiently small,

$$i) F(\mu_1, \mu_2) = 0 \text{ is a unique curve in the plane } \mu_1\mu_2, \text{ given by}$$

$$\mu_2 = -\frac{b}{a}\mu_1(1 + O(\mu_1)),$$

ii) if $\Delta = b^2 - ac > 0$, then $G(\mu_1, \mu_2) = 0$ is a union of two curves passing through the origin $O(0, 0)$ and having the forms

$$\mu_2 = e_1\mu_1(1 + O(\mu_1)) \text{ and } \mu_2 = e_2\mu_1(1 + O(\mu_1)), \quad (9)$$

where $e_1 = \frac{b+\sqrt{\Delta}}{a}$ and $e_2 = \frac{b-\sqrt{\Delta}}{a}$, and

iii) if $\Delta = b^2 - ac < 0$, then $G(\mu_1, \mu_2) = 0$ is satisfied only at $(0, 0)$ and $\text{sign}(G(\mu_1, \mu_2)) = \text{sign}(a)$ for all $(\mu_1, \mu_2) \in D$.

PROOF. i) Since $F(0, 0) = 0$ and $\frac{\partial F}{\partial \mu_2}(0, 0) = a \neq 0$, the IFT yields the conclusion. The function $\mu_2 = -\frac{b}{a}\mu_1(1 + O(\mu_1))$ exists and is unique for all $|\mu_1|$ sufficiently small.

ii) The proof is more involved in this case. $G(\mu_1, \mu_2) = 0$ is equivalent to

$$a\mu_2^2 - 2b\mu_1\mu_2(1 + O(|\mu|)) + c\mu_1^2(1 + O(|\mu|)) = 0. \quad (10)$$

Notice that $\frac{1+O(|\mu|)}{1+O(|\mu|)} = 1 + O(|\mu|)$. Then, solving for μ_2 in (10) when $\Delta > 0$, we get an implicit equation

$$H_{\pm}(\mu_1, \mu_2) \stackrel{\text{def}}{=} \mu_2 - \frac{\mu_1}{a} \left(b(1 + O(|\mu|)) \pm \sqrt{\Delta}(1 + O(|\mu|)) \right) = 0.$$

But $H_{\pm}(0, 0) = 0$ and $\frac{\partial H_{\pm}}{\partial \mu_2}(0, 0) = 1 \neq 0$ for all $O(|\mu|)$. Notice that $O(|\mu|) = \sum_{i+j \geq 1} c_{ij}\mu_1^i\mu_2^j$ contains terms both in μ_1 but also in μ_2 . The conclusion follows now from the IFT and Taylor theorem. Notice that $e_{1,2} \neq 0$ from $ac \neq 0$.

iii) It is clear that, the implicit functions $H_{\pm}(\mu_1, \mu_2)$ do not exist when $\Delta < 0$. Thus $G(\mu_1, \mu_2) \neq 0$ for all $(\mu_1, \mu_2) \neq (0, 0)$ with $|\mu| < \varepsilon$. Moreover, since $G(\mu_1, \mu_2)$ is a quadratic equation in μ_2 , it follows that $\text{sign}(G(\mu_1, \mu_2)) = \text{sign}[a(1 + O(|\mu|))] = \text{sign}(a)$ for $|\mu|$ sufficiently small. ■

Remark 2.6. If $b^2 - ac = 0$, the discriminant of the equation $G(\mu_1, \mu_2) = 0$ in μ_2 is undefined, being of the form $|\mu_1| \sqrt{O(|\mu|)}$. Thus, the existence of curves of equation $G(\mu_1, \mu_2) = 0$ cannot be decided. A further study could be performed in this case but this is beyond the purpose of this article.

The following bifurcation curves T_1 and T_2 are important for obtaining bifurcation diagrams to describe the behavior of the system (4), namely

$$T_1 = \left\{ (\mu_1, \mu_2) \in \mathbb{R}^2 \mid \mu_2 = \frac{\delta}{\theta}\mu_1 + O(\mu_1^2), \frac{\mu_1}{\theta} > 0 \right\} \quad (11)$$

and

$$T_2 = \left\{ (\mu_1, \mu_2) \in \mathbb{R}^2 \mid \mu_2 = \frac{1}{\gamma}\mu_1 + O(\mu_1^2), \mu_1 > 0 \right\}. \quad (12)$$

T_1 is defined by $\xi_2 = 0$ while T_2 by $\xi_1 = 0$, where $\xi_{1,2}$ are given by (8) and correspond to $E_3(\xi_1, \xi_2)$.

Remark 2.7. 1) The eigenvalues of $E_1(\xi_1, 0)$ are $\lambda_1^{E_1} = \mu_1 - 2\theta\xi_1 + 3N\xi_1^2$ and $\lambda_2^{E_1} = \mu_2 - \delta\xi_1 + S\xi_1^2$, which in their lowest terms become $\lambda_1^{E_1} = -\mu_1 + O(\mu_1^2)$ and $\lambda_2^{E_1} = \mu_2 - \frac{1}{\theta}\delta\mu_1 + O(\mu_1^2)$, since $\xi_1 = \frac{1}{\theta}\mu_1 + O(\mu_1^2)$.

2) The eigenvalues of $E_2(0, \xi_2)$ are $\lambda_1^{E_2} = \mu_1 + \gamma\xi_2$ and $\lambda_2^{E_2} = \mu_2 + 2\xi_2 + 3P\xi_2^2$, that is, $\lambda_1^{E_2} = \mu_1 - \gamma\mu_2 + O(\mu_2^2)$ and $\lambda_2^{E_2} = -\mu_2 + O(\mu_2^2)$, with $\xi_2 = -\mu_2 + O(\mu_2^2)$.

3) The eigenvalues of O are $\mu_{1,2}$.

Theorem 2.8. *Assume $\theta\delta \neq 0$ and $\theta - \gamma\delta \neq 0$. Then T_1 is a transcritical bifurcation curve for all $|\mu|$ sufficiently small.*

Proof. When $(\mu_1, \mu_2) \in T_1$, the points $E_3(\xi_1, \xi_2)$ and $E_1(\xi_1, 0)$ coalesce (collide), becoming a double non-hyperbolic singular point on T_1 , with one eigenvalue $\lambda_2^{E_1} = 0$ and the other $\lambda_1^{E_1} = -\mu_1 + O(\mu_1^2)$. Indeed, $\xi_2 = 0$ in (6) yields $\mu_2 - \delta\xi_1 + S\xi_1^2 = 0$, thus, by Remark 2.7, $\lambda_2^{E_1} = 0$. We notice that $E_1 \in Q1$ if $\frac{\mu_1}{\theta} > 0$, since $\xi_1 = \frac{1}{\theta}\mu_1 + O(\mu_1^2)$.

We apply in the following Sotomayor's theorem (see [10]). To this end, write first the system (4) in the form $\frac{d\xi}{dt} = f(\xi, \mu)$, where $\xi = (\xi_1, \xi_2)$, $\mu = (\mu_1, \mu_2)$ and $f = (f_1, f_2)$.

At $E_1(\xi_1, 0)$ with $\mu_1 - \theta\xi_1 + N\xi_1^2 = 0$, denote also by $\xi_0 = (\xi_1, 0)$ and $\mu_0 = (\mu_1, \mu_2) \in T_1$, with $\mu_1 \neq 0$. Since $E_3(\xi_1, \xi_2)$ collides to $E_1(\xi_1, 0)$ on T_1 , by (6), ξ_1 satisfies also $\mu_2 - \delta\xi_1 + S\xi_1^2 = 0$. Then, $f(\xi_0, \mu_0) = (0, 0)$ and the Jacobian matrix of f at (ξ_0, μ_0) is

$$A = Df(\xi_0, \mu_0) = \begin{pmatrix} \theta\xi_1 - 2\mu_1 & \xi_1(\gamma - M\xi_1) \\ 0 & 0 \end{pmatrix}.$$

The eigenvector of A , respectively A^T , corresponding to the null eigenvalue $\lambda_2^{E_1} = 0$ are $v = \begin{pmatrix} \frac{\gamma\xi_1 - M\xi_1^2}{2\mu_1 - \theta\xi_1} \\ 1 \end{pmatrix}$, respectively, $w = \begin{pmatrix} 0 \\ 1 \end{pmatrix}$. Notice that $v = \begin{pmatrix} \frac{\gamma}{\theta} + O(\mu_1) \\ 1 \end{pmatrix}$ is well-defined for all $|\mu|$ sufficiently small with $\mu_1 \neq 0$. Assume μ_1 is fixed with $\frac{\mu_1}{\theta} > 0$ and consider μ_2 as the bifurcation parameter. Denote by $f_{\mu_2} = \begin{pmatrix} \frac{\partial f_1}{\partial \mu_2} \\ \frac{\partial f_2}{\partial \mu_2} \end{pmatrix}$ and $D^2f(\xi, \mu)(v, v) = \begin{pmatrix} d^2f_1(\xi, \mu)(v, v) \\ d^2f_2(\xi, \mu)(v, v) \end{pmatrix}$, where $d^2f_{1,2}(\xi, \mu)(v, v)$ are the differentials of second order of the functions $f_{1,2}$. Since $\frac{\partial f_2}{\partial \mu_2}(\xi_0, \mu_0) = 0$, it follows that $C_1 = w^T \cdot f_{\mu_2}(\xi_0, \mu_0) = 0$. If Df_{μ_2} denotes the Jacobian matrix in variables ξ_1 and ξ_2 of f_{μ_2} , we get

$$C_2 = w^T [Df_{\mu_2}(\xi_0, \mu_0)(v)] = 1 + O(\mu_1).$$

Finally, we find

$$C_3 = w^T [D^2f(\xi_0, \mu_0)(v, v)] = 2\frac{\theta - \gamma\delta}{\theta} + O(\mu_1).$$

Thus, $C_2 \neq 0$ and $C_3 \neq 0$ for all $|\mu|$ sufficiently small, which complete the proof. ■

Remark 2.9. *A similar scenario to T_1 occurs for T_2 . Indeed, if $(\mu_1, \mu_2) \in T_2$, then $E_3(\xi_1, \xi_2)$ and $E_2(0, \xi_2)$ coalesce. By (6), their joint eigenvalues are $\lambda_1^{E_2} = 0$ and $\lambda_2^{E_2} = -\mu_2 + O(\mu_2^2)$. $E_2 \in Q1$ if $\mu_2 < 0$.*

Denote by $X_+ = \{(\mu_1, 0), \mu_1 > 0\}$, $X_- = \{(\mu_1, 0), \mu_1 < 0\}$, $Y_+ = \{(0, \mu_2), \mu_2 > 0\}$ and $Y_- = \{(0, \mu_2), \mu_2 < 0\}$, the four half-axes in the parametric plane $\mu_1\mu_2$.

On $X_+ \cup X_-$, the point $O(0, 0)$ collides to $E_2(0, \xi_2)$ and have the eigenvalues 0 and μ_1 , while on $Y_+ \cup Y_-$, $O(0, 0)$ collides to $E_1(\xi_1, 0)$ and have the eigenvalues 0 and μ_2 .

Remark 2.10. *One can show similarly to T_1 that T_2 , X_+ , X_- , Y_+ and Y_- are all transcritical bifurcation curves. Knowing that the system (4) undergoes a transcritical bifurcation when the parameter (μ_1, μ_2) crosses these curves is important in determining the phase portraits on the curves, which represent borders of different regions in the parametric plane. This will be exploited in the next section.*

The characteristic polynomial at an equilibrium point (ξ_1, ξ_2) of the system (4) has the form $P(\lambda) = \lambda^2 - 2p\lambda + L$. When (ξ_1, ξ_2) is an equilibrium point of type E_3 , that is, its coordinates satisfy (6), then p and L at (ξ_1, ξ_2) become

$$p = \frac{1}{2}\xi_2 - \frac{1}{2}\theta\xi_1 + N\xi_1^2 - \frac{1}{2}M\xi_1\xi_2 + P\xi_2^2, \quad (13)$$

$$L = -\xi_1\xi_2 (\theta - \gamma\delta + c_{11}\xi_1 + c_{12}\xi_2 - 4NP\xi_1\xi_2 - 2MS\xi_1^2 + 2MP\xi_2^2), \quad (14)$$

where $c_{11} = M\delta - 2N + 2S\gamma$ and $c_{12} = M + 2P\theta$.

Consider that the eigenvalues of $E_3(\xi_1, \xi_2)$, which are roots of $P(\lambda)$, are of the form

$$\lambda_{1,2} = p \pm \sqrt{q}. \quad (15)$$

Then $\lambda_1\lambda_2 = L$ and $q = p^2 - L$ lead to

$$\begin{aligned} q = & \frac{1}{4}(\theta^2\xi_1^2 + 2\xi_1\xi_2(\theta - 2\gamma\delta) + \xi_2^2) - N\theta\xi_1^3 + \frac{1}{2}(2N + M\theta + 2c_{11})\xi_1^2\xi_2 + \frac{1}{2}(M + 2P\theta)\xi_1\xi_2^2 \\ & + P\xi_2^3 + N^2\xi_1^4 - (N + 2S)M\xi_1^3\xi_2 + \frac{1}{4}(M^2 - 8NP)\xi_1^2\xi_2^2 + MP\xi_1\xi_2^3 + P^2\xi_2^4. \end{aligned} \quad (16)$$

Using the expressions of $\xi_{1,2}$ at E_3 given in (8), we can write

$$\begin{aligned} p &= \frac{\delta - \theta}{2(\theta - \gamma\delta)}\mu_1(1 + O(|\mu|)) - \frac{\theta - \gamma\theta}{2(\theta - \gamma\delta)}\mu_2(1 + O(|\mu|)), \\ q &= \frac{1}{4(\theta - \gamma\delta)^2}(a\mu_2^2(1 + O(|\mu|)) - 2b\mu_1\mu_2(1 + O(|\mu|)) + c\mu_1^2(1 + O(|\mu|))), \end{aligned} \quad (17)$$

where

$$a = \theta^2(\gamma + 1)^2 - 4\theta\gamma^2\delta, \quad b = -2\delta^2\gamma^2 + \theta(\theta - \delta)\gamma + \theta(\theta + \delta) \quad \text{and} \quad c = (\theta + \delta)^2 - 4\gamma\delta^2. \quad (18)$$

Notice that $c \neq 0$ because $\theta\delta \neq 0$ and $\gamma < 0$. By (14), the product $\lambda_1\lambda_2$ is of the form

$$\lambda_1\lambda_2 = -(\theta - \gamma\delta)\xi_1\xi_2(1 + O(|\mu|)). \quad (19)$$

Remark 2.11. *By Lemma 2.5, we can approximate E_3 , p and q by their lowest terms, whenever they satisfy the Lemma's conditions. The qualitative behavior of the system does not change by this approximation. For example, the curve $\mu_2 = e_1\mu_1(1 + O(\mu_1))$ for $e_1 \neq 0$ is approximated by $\mu_2 = e_1\mu_1$. In this approximation, $\text{sign}[G(\mu_1, \mu_2)] = \text{sign}[G_0(\mu_1, \mu_2)]$ for $|\mu|$ sufficiently small, where $G_0(\mu_1, \mu_2) = a\mu_2^2 - 2b\mu_1\mu_2 + c\mu_1^2$.*

When $a \neq 0$, the discriminant in its lowest terms of the equation $q = 0$ in variable μ_2 is

$$\Delta = b^2 - ac = -4\gamma\delta(\theta - \gamma\delta)^3\mu_1^2. \quad (20)$$

Theorem 2.12. *1) Assume $\theta - \gamma\delta < 0$. Then E_3 is stable (node or focus) on $p < 0$ and unstable on $p > 0$. In particular, if $\delta > 0$ then E_3 is an unstable node.*

2) Assume $\theta - \gamma\delta > 0$. Then E_3 is a saddle.

PROOF. It follows from (13) that $p > 0$ if $\theta - \gamma\delta \neq 0$ and $\theta < 0$, whenever $E_3(\xi_1, \xi_2)$ satisfies $\xi_{1,2} > 0$. In its lowest terms, p reads

$$p = -\frac{1}{2(\theta - \gamma\delta)} (\theta(\mu_1 - \gamma\mu_2) - (\delta\mu_1 - \theta\mu_2)).$$

1) When $\theta - \gamma\delta < 0$, $E_3\left(\frac{\mu_1 - \gamma\mu_2}{\theta - \gamma\delta}, \frac{\delta\mu_1 - \theta\mu_2}{\theta - \gamma\delta}\right)$ exists in the first quadrant $Q1$ defined by $\xi_1 > 0$ and $\xi_2 > 0$, whenever (μ_1, μ_2) lies in the region

$$R_1 = \{(\mu_1, \mu_2) \in \mathbb{R}^2 \mid \mu_1 - \gamma\mu_2 < 0, \delta\mu_1 - \theta\mu_2 < 0\}.$$

It follows from (19) that $\lambda_1\lambda_2 > 0$ on R_1 . Thus, E_3 is stable on $p < 0$ (node or focus), respectively, unstable on $p > 0$ (node or focus). Assume further:

i) $\delta > 0$. Then $\theta < \gamma\delta < 0$, $\Delta = -4\gamma\delta(\theta - \gamma\delta)^3 < 0$, $a > 0$ and $p > 0$, since $\gamma < 0$. Thus $q > 0$ and E_3 is an unstable node.

ii) $\delta < 0$. Then $\Delta > 0$ and $q = 0$ give rise to two bifurcation curves, denoted by C_1 and C_2 and given in (9), which determine on R_1 when E_3 changes from a node to a focus or vice versa; $\lambda_1\lambda_2 > 0$.

2) In the second case $\theta - \gamma\delta > 0$, $E_3 \in Q1$ when (μ_1, μ_2) lies in the region

$$R_2 = \{(\mu_1, \mu_2) \in \mathbb{R}^2 \mid \mu_1 - \gamma\mu_2 > 0, \delta\mu_1 - \theta\mu_2 > 0\}.$$

From (19), we deduce $\lambda_1\lambda_2 < 0$. Therefore $\lambda_{1,2} \in \mathbb{R}$ and $q > 0$. We conclude that E_3 is a saddle. ■

Taking into account the behavior of E_3 described in the above theorem, we can study easier the Hopf bifurcation in (4) at E_3 .

Theorem 2.13. 1) If $\theta < 0$ or $0 < \gamma\delta < \theta$ or $\gamma\delta < 0 < \theta$, the system (4) does not undergo a Hopf bifurcation at E_3 .

2) A Hopf bifurcation occurs at E_3 provided that $0 < \theta < \gamma\delta$.

PROOF. 1) A Hopf bifurcation cannot occur at E_3 when $\theta < 0$ either on R_1 or R_2 because $p \neq 0$. Assume further $\theta > 0$. Then $p = 0$ along the curve

$$H = \left\{ (\mu_1, \mu_2) \mid \mu_2 = \mu_1 \frac{\theta - \delta}{\theta(\gamma - 1)} + O(\mu_1^2), \theta \neq \delta \right\} \quad (21)$$

and $q = \mu_1^2 \frac{\theta - \gamma\delta}{\theta(\gamma - 1)^2} + O(\mu_1^3)$ on H ; $\gamma < 0$. If in addition $\gamma\delta < \theta$, then $q > 0$ on H . Thus, a Hopf bifurcation cannot occur since the eigenvalues $\lambda_{1,2}$ are not purely imaginary on H .

We still need to consider the case $\theta = \delta$. Then p in its lowest terms is an expression of the form

$$p = -\frac{1}{2}\mu_2 + \frac{1}{2}c_n\mu_1^n$$

with $n \geq 2$ and $c_n \neq 0$. Thus, $p = 0$ leads to $\mu_2 = c_n\mu_1^n$. Calculating now the expression of q for $\mu_2 = c_n\mu_1^n$ we find $q = \frac{\mu_1^2}{1-\gamma}(1 + O(\mu_1)) > 0$ for $|\mu_1|$ small enough with $\mu_1 \neq 0$. It concludes that a Hopf bifurcation can not occur at $\theta = \delta$.

2) If $0 < \theta < \gamma\delta$ then $\lambda_{1,2} = \pm\omega i$ on H , with $\omega = \frac{\mu_1}{\theta(1-\gamma)}\sqrt{(\gamma\delta - \theta)\theta} > 0$ in their lowest terms.

One can show that E_3 is defined on $\mu_1 > 0$ in this case, Figure 8 (VII). Since $\frac{\partial p}{\partial \mu_2}\Big|_H = \frac{\theta(\gamma-1)}{2(\theta-\gamma\delta)\delta} \neq 0$, a Hopf bifurcation (degenerate or not) occurs at E_3 . We notice that $\theta \neq \delta$ in this case because $\theta > 0$ and $\delta < 0$.

When the bifurcation is degenerate with respect to the first Lyapunov coefficient (that is, $l_1(0) = 0$), other codim k bifurcations may arise with $k \geq 2$. In case of non-degeneracy of the Hopf bifurcation, a periodic orbit (limit cycle) arises around E_3 , but when the bifurcation becomes degenerate (e.g. Bautin bifurcation) more limit cycles are typically born around E_3 with the increasing of the codimension. ■

3 Bifurcation diagrams

We perform in this section a complete analysis of the bifurcation diagrams when the parameters δ, γ, θ vary with $\theta\delta \neq 0$, $\theta - \gamma\delta \neq 0$ and $\gamma < 0$. In order to obtain the diagrams and distinct generic phase portraits of the system (4), we will use the cases and results obtained in Theorems 2.12-2.13.

Case 1. Consider the first inequality $\theta - \gamma\delta < 0$. More different cases arise here in order to obtain all configurations of bifurcation diagrams.

Case 1.a) Assume in addition $\delta > 0$, that is, $\theta < \gamma\delta < 0$. Then (13), (18), (20) yield $p > 0$, $\Delta < 0$, $a > 0$ and $q > 0$. The equilibrium point E_3 is an unstable node in this case, whenever it exists in $Q1$. The bifurcation diagram is depicted in Figure 1 (I).

Let us describe the phase portraits on the bifurcation curves $T_{1,2}$, $X_{+,-}$ and $Y_{+,-}$ in the first diagram (I). We will exemplify this on the curve T_1 . The description is similar for the other curves and the next diagrams. Since T_1 is a transcritical bifurcation curve and the colliding points E_3 and $E_1(\frac{1}{\theta}\mu_1 + O(\mu_1^2), 0)$ have the eigenvalues 0 and $-\mu_1 + O(\mu_1^2)$, the phase portrait of the system (4) is known when $(\mu_1, \mu_2) \in T_1$ and given in Figure 2(T1). Notice that $\theta < 0$ and, from $\lambda_1\lambda_2 = -(\theta - \gamma\delta)\xi_1\xi_2(1 + O(|\mu|))$ given in (19), $E_3(\xi_1, \xi_2)$ is a saddle when (μ_1, μ_2) lies in the region 1 from Figure 1 (I), since $\xi_1 > 0$ and $\xi_2 < 0$, see Figure 2(1). After (μ_1, μ_2) crosses T_1 into the region 6, $E_3(\xi_1, \xi_2)$ becomes an unstable node and lies in the first quadrant, Figure 2(6).

Comparing the two phase portraits from Figures 2(1)-2(T1), we observe they coincide in the first quadrant. As a conclusion we have the next remark.

Remark 3.1. Denote by T_1^{vir} the region to the left or right of T_1 where E_3 is virtual (i.e. $E_3 \notin Q1$). For example, T_1^{vir} is the region 1 in Figure 1 (I). Then, the behaviour of the system (4) when $(\mu_1, \mu_2) \in T_1$ coincides in the first quadrant $Q1$ to the one for $(\mu_1, \mu_2) \in T_1^{vir}$. In other words, the phase portrait on T_1 is the same (in $Q1$) as the one to the left or right of T_1 where E_3 is virtual. The same scenario applies for T_2 and all the other bifurcation curves $X_{+,-}$ and $Y_{+,-}$, with the difference that E_3 is replaced correspondingly with E_1 or E_2 , since in these latter cases, E_1 or E_2 collide to O . This rule applies for all bifurcation diagrams from this section.

Remark 3.2. On the curves $C_1 - C_4$, which separate a node from a focus, E_3 is a node (since $q = 0$), thus, the phase portrait on each of these curves coincides to the phase portrait on the left or right of the curves where E_3 is a node.

Case 1.b) Consider $\theta - \gamma\delta < 0$, $\delta < 0$, and $\theta < 0$. Therefore $p > 0$ which, in turn, implies that a Hopf bifurcation cannot occur at E_3 . From $\Delta > 0$ and Lemma 2.5, two bifurcation curves arise from $q = 0$, namely

$$C_1 : \mu_2 = e_1\mu_1 \text{ and } C_2 : \mu_2 = e_2\mu_1, \quad (22)$$

where a, b, c are given by (18). The two curves $C_{1,2}$ control the sign of q . Denote by $m_{C_1} = e_1$, $m_{C_2} = e_2$, $m_{T_1} = \frac{\delta}{\theta}$ and $m_{T_2} = \frac{1}{\gamma}$ the slopes of the straight lines C_1 , C_2 , T_1 (11) and T_2 (12) respectively. Notice that $m_{T_1} > 0$ and $m_{T_2} < 0$. To determine the relative position of these slopes on

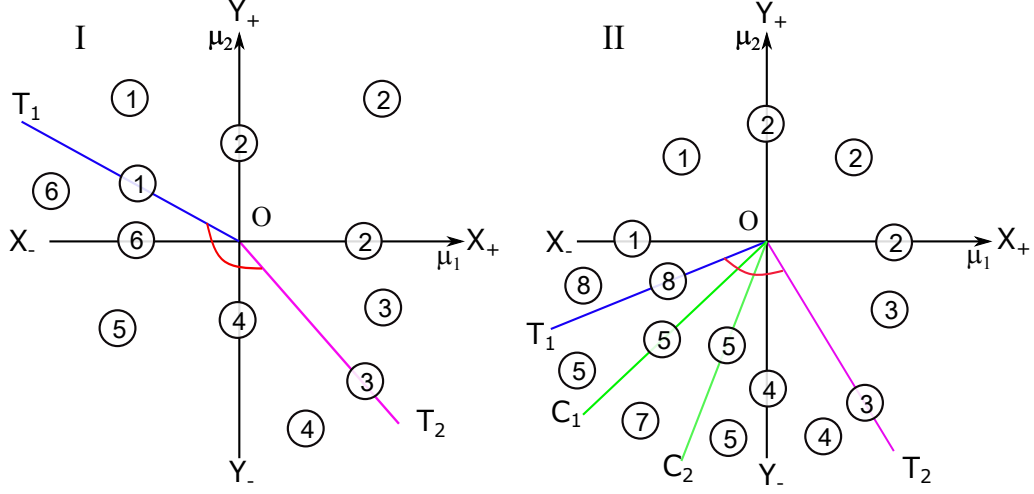


Figure 1: Bifurcation diagrams of system (4) for: $\theta - \gamma\delta < 0, \delta > 0$ (I), respectively, $\theta - \gamma\delta < 0, \delta < 0, \theta < 0, a > 0$ and $-1 < \gamma < 0$ (II).

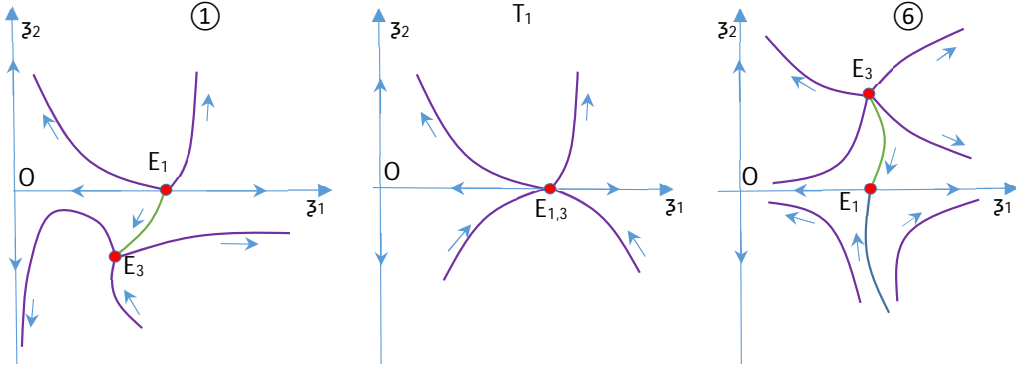


Figure 2: The behavior of the system (4) when (μ_1, μ_2) crosses T_1 in the first bifurcation diagram (I).

the real axis, we need to know the signs of the following expressions:

$$P_1 = m_1 \cdot m_2 = \frac{(\theta - \gamma\delta)^2}{\gamma^2 a}, \quad S_1 = m_1 + m_2 = \frac{-4(\theta - \gamma\delta)\theta}{a} \left(\frac{\gamma + 1}{2\gamma} - \gamma \frac{\delta}{\theta} \right) \quad (23)$$

and

$$P_2 = m'_1 \cdot m'_2 = \frac{(\theta - \gamma\delta)^2}{a}, \quad S_2 = m'_1 + m'_2 = \frac{4(\theta - \gamma\delta)\theta\gamma}{a} \left(\frac{\gamma + 1}{2\gamma} - \frac{\delta}{\theta} \right), \quad (24)$$

where $m_i = e_i - \frac{1}{\gamma}$ and $m'_i = e_i - \frac{\delta}{\theta}$, $i = 1, 2$.

Taking into account that the sign of $a = 4\gamma^2\theta^2 \left[\left(\frac{\gamma+1}{2\gamma} \right)^2 - \frac{\delta}{\theta} \right]$ is undetermined in this subcase, we

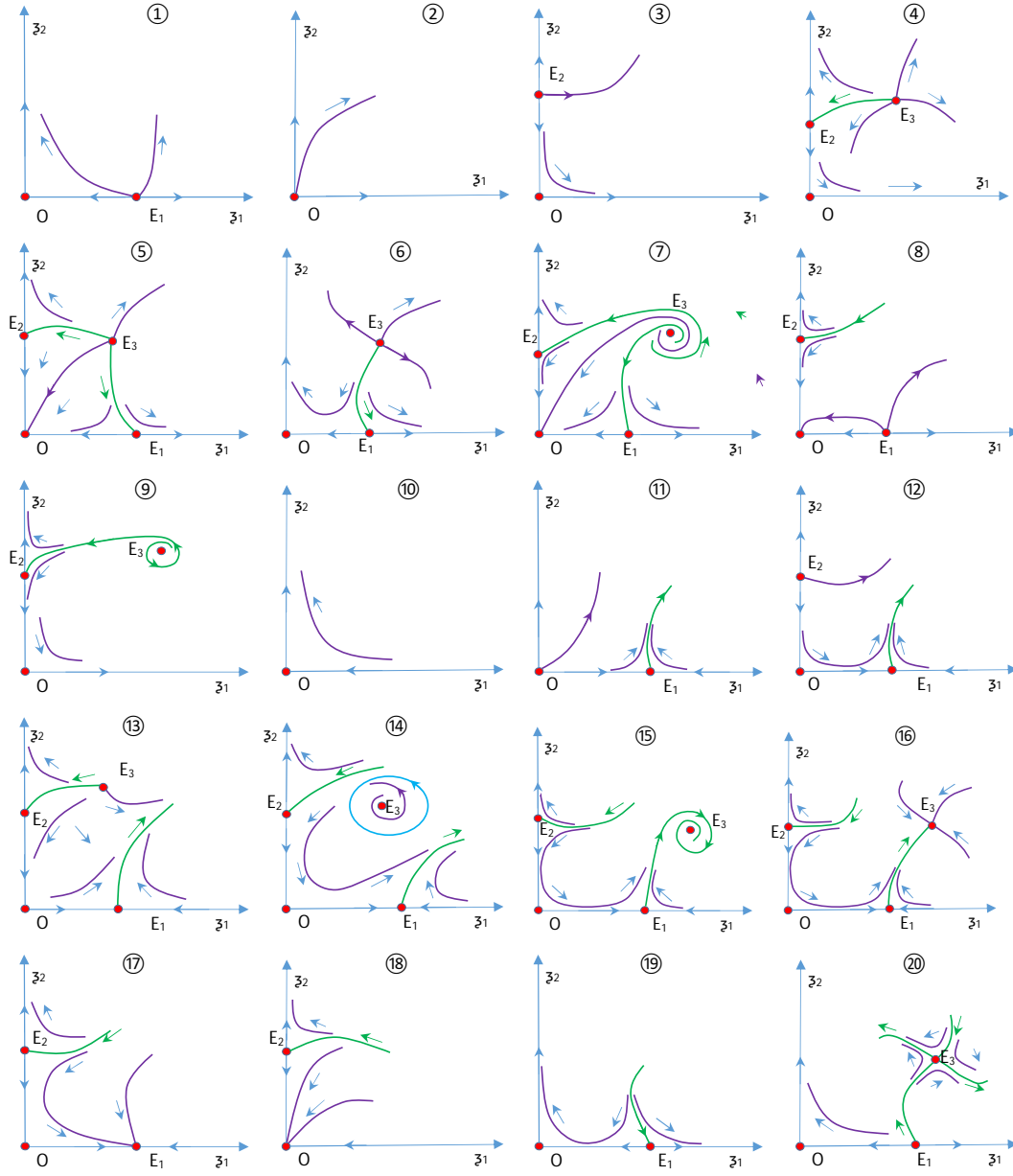


Figure 3: Phase portraits corresponding to different regions of the bifurcation diagrams.

obtain the following possible situations.

(i) Consider $a > 0$, that is, $0 < \frac{\delta}{\theta} < \left(\frac{\gamma+1}{2\gamma}\right)^2$ and $\gamma \neq -1$.

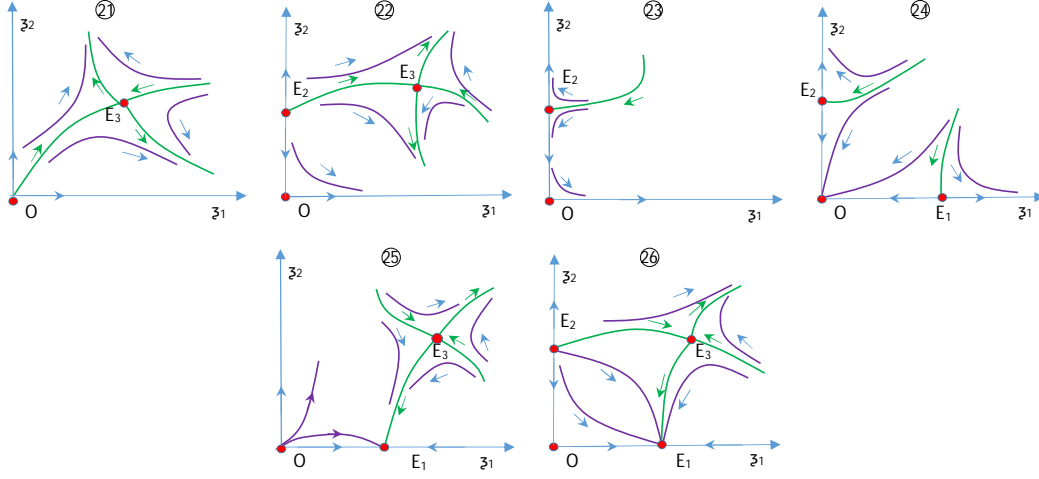


Figure 4: Phase portraits corresponding to different regions of the bifurcation diagrams.

If $-1 < \gamma < 0$, then from (24) we deduce $P_2 > 0$ and $S_2 > 0$. Therefore we have

$$\frac{1}{\gamma} < 0 < \frac{\delta}{\theta} < e_1 < e_2.$$

The bifurcation diagram is depicted in Figure 1 (II).

If $\gamma < -1$, then from (23) we deduce $P_1 > 0$ and $S_1 < 0$. Therefore we have

$$e_1 < e_2 < \frac{1}{\gamma} < 0 < \frac{\delta}{\theta}.$$

The bifurcation diagram is depicted in Figure 5 (III).

(ii) Assume $a < 0$, that is, $\frac{\delta}{\theta} > \left(\frac{\gamma+1}{2\gamma}\right)^2$ for all $\gamma < 0$. Hence $e_2 < 0 < e_1$. Moreover, $P_1 < 0$ and $P_2 < 0$, whence

$$e_2 < \frac{1}{\gamma} < 0 < \frac{\delta}{\theta} < e_1.$$

The bifurcation diagram is depicted in Figure 5 (IV).

(iii) Finally, let $a = 0$, that is, $\theta = \frac{4\gamma^2\delta}{(1+\gamma)^2}$; $\gamma \neq -1$ in this case because, otherwise, $a = -4\theta\delta \neq 0$ at $\gamma = -1$. Hence $b = \frac{2\delta^2\gamma^2(1-\gamma)^3}{(1+\gamma)^3} \neq 0$, while $c \neq 0$ for all $\theta\delta \neq 0$ and $\gamma < 0$. The sign of q cannot be concluded in this case from (17) because a term in μ_2^n with $n \geq 2$ is missing. Therefore, we have to use terms up to order three in the general expression of q given by (16) in order to determine its leading (lowest) terms. At $\theta = \frac{4\gamma^2\delta}{(1+\gamma)^2}$, we obtain from (16) that q in its lowest terms reads

$$q = c\mu_1^2(1 + O_1(|\mu|)) - 2b\mu_1\mu_2(1 + O_2(|\mu|)) + d\mu_2^3(1 + O_3(|\mu|)), \quad (25)$$

where $c = \frac{4\gamma^2+3\gamma+1}{4\gamma^2(1-\gamma)}$, $b = -\frac{\gamma+1}{2(\gamma-1)}$, $d = \frac{4\gamma(\gamma+1)}{\delta^2(\gamma-1)^6} ((2S - N)\gamma^4 + d_{31}\gamma^3 + d_{21}\gamma^2 + d_{11}\gamma + M\delta - N)$, respectively, $d_{31} = 6S - 4N + 3M\delta$, $d_{21} = 16P\delta^2 + 7M\delta - 6N + 6S$ and $d_{11} = 2S - 4N + 5M\delta$.

The sign of q from (25) can be determined. Applying a method based on IFT as in Lemma 2.5, the equation $q = 0$ is satisfied along two bifurcation curves, given by

$$C_3 = \left\{ (\mu_1, \mu_2) \mid \mu_1 = \frac{2b}{c} \mu_2 + O(\mu_2^2) \right\} \quad (26)$$

and

$$C_4 = \left\{ (\mu_1, \mu_2) \mid \mu_1 = -d \frac{\gamma-1}{\gamma+1} \mu_2^2 + O(\mu_2^3) \right\} \quad (27)$$

for all $\gamma \neq -1$. The two curves determine in the parametric plane the sign of q for all $|\mu|$ sufficiently small. Notice that C_4 is tangent to the μ_2 -axis at O .

Two cases arise, namely $b < 0$ (iff $\gamma < -1$) and then $\frac{1}{\gamma} > \frac{c}{2b}$ (see Figures 6, V(a)-(b)) and $b > 0$ (iff $-1 < \gamma < 0$) and then $\frac{\delta}{\theta} < \frac{c}{2b}$ (see Figures 7, VI(a)-(b)), respectively. Notice that $\frac{c}{2b} = \frac{4\gamma^2+3\gamma+1}{4(\gamma+1)\gamma^2}$, respectively, $\frac{1}{\gamma} - \frac{c}{2b} = \frac{\gamma-1}{4\gamma^2(\gamma+1)}$ and $\frac{\delta}{\theta} - \frac{c}{2b} = \frac{\gamma-1}{4(\gamma+1)}$. In each of the two cases we considered that d can be either positive or negative. When $d = 0$, a further analysis is required to determine the sign of q . This will need all terms in the general expression of q from (16).

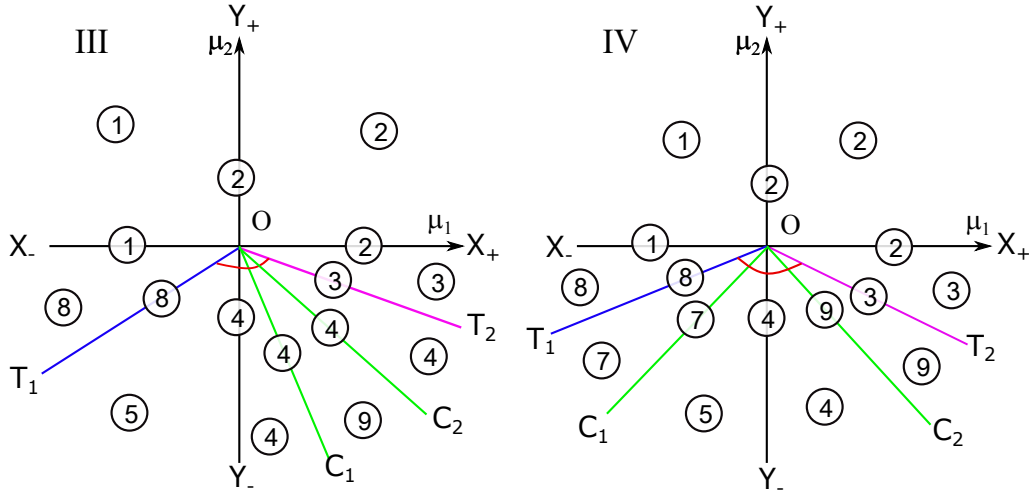


Figure 5: Bifurcation diagrams of system (4) for: $\theta - \gamma\delta < 0$, $\delta < 0$, $\theta < 0$, and $a > 0$ and $\gamma < -1$ (III), respectively, $\theta - \gamma\delta < 0$, $\delta < 0$, $\theta < 0$ and $a < 0$ (IV).

Case 1.c) Consider $\theta - \gamma\delta < 0$, $\delta < 0$, and $\theta > 0$. Thus $0 < \theta < \gamma\delta$. In this case, a Hopf bifurcation occurs at E_3 . Indeed, $p = 0$ along the bifurcation curve

$$H = \left\{ (\mu_1, \mu_2) \mid \mu_2 = \frac{\theta - \delta}{\theta(\gamma - 1)} \mu_1 + O(\mu_1^2), \theta \neq \delta \right\}$$

and $\frac{\partial p}{\partial \mu_2} \Big|_H = \frac{(\gamma-1)\theta}{2(\theta-\gamma\delta)} \neq 0$. Notice that $\theta \neq \delta$ is satisfied in this case. Then $q = \mu_1^2 \frac{\theta-\gamma\delta}{\theta(\gamma-1)^2} < 0$ on H and the eigenvalues associated to the equilibrium point E_3 are $\lambda_{1,2} = \pm i\sqrt{-q}$ along the curve H . The

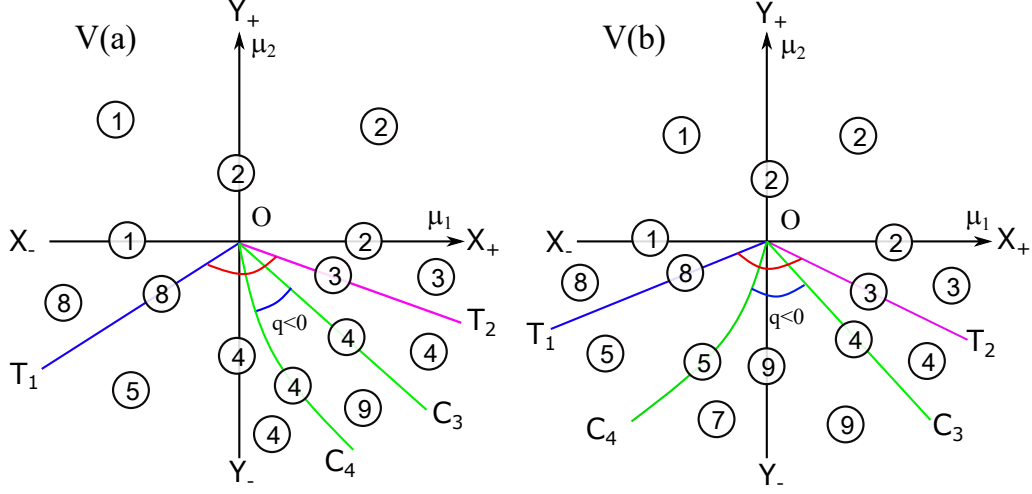


Figure 6: Bifurcation diagrams of system (4) when $\theta - \gamma\delta < 0$, $\delta < 0$, $\theta < 0$, $a = 0$, $\gamma < -1$, respectively, $d < 0$ on V(a) and $d > 0$ on V(b).

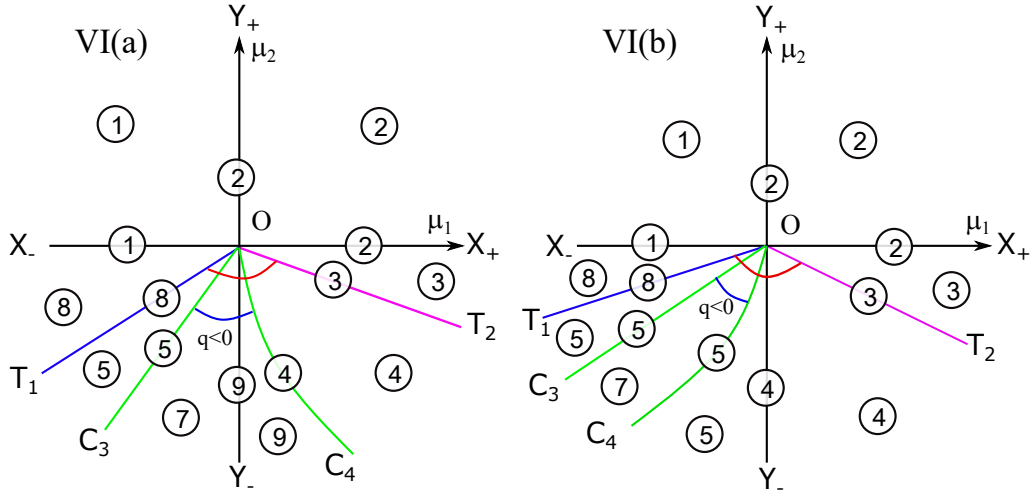


Figure 7: Bifurcation diagrams of system (4) when $\theta - \gamma\delta < 0$, $\delta < 0$, $\theta < 0$, $a = 0$, $-1 < \gamma < 0$, respectively, $d > 0$ on VI(a) and $d < 0$ on VI(b).

following order is obtained in this case, namely:

$$\frac{\delta}{\theta} < e_1 < \frac{\theta - \delta}{\theta(\gamma - 1)} < e_2 < \frac{1}{\gamma} < 0. \quad (28)$$

Indeed, from $\gamma < 0$ we have that $\Delta = -4\gamma\delta(\theta - \gamma\delta)^3 > 0$, $a > 0$ and the equation $a\mu_2^2 - 2b\mu_1\mu_2 + c$

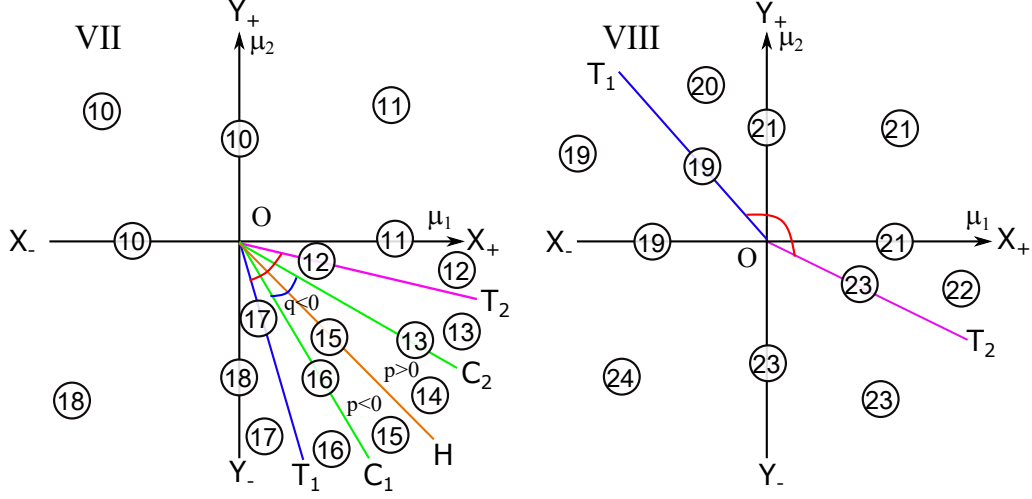


Figure 8: Parametric portrait of system (4) when $\theta - \gamma\delta < 0$, $\delta < 0$, and $\theta > 0$ (VII), respectively, $\theta - \gamma\delta > 0$, $\delta > 0$, and $\theta < 0$ (VIII).

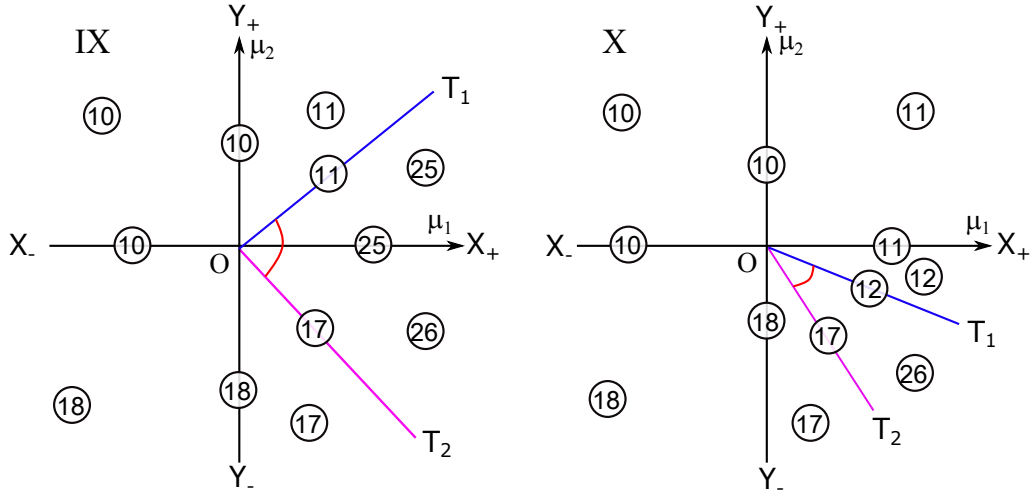


Figure 9: Parametric portrait of system (4) when $\theta - \gamma\delta > 0$, $\delta > 0$, and $\theta > 0$ (IX), respectively, $\theta - \gamma\delta > 0$ and $\delta < 0$ (X).

$\mu_1^2 = 0$ in μ_2 has two roots $\mu_2 = e_1\mu_1$ and $\mu_2 = e_2\mu_1$, where $e_1 = \frac{b-\sqrt{\Delta}}{a}$ and $e_2 = \frac{b+\sqrt{\Delta}}{a}$, with $e_1 < e_2$. Therefore we deduce $m_1 \cdot m_2 > 0$, $m'_1 \cdot m'_2 > 0$ and $\left(e_1 - \frac{\theta-\delta}{\theta(\gamma-1)}\right) \left(e_2 - \frac{\theta-\delta}{\theta(\gamma-1)}\right) = \frac{4(\theta-\gamma\delta)^3}{\theta(\gamma-1)^2 a} < 0$. Also we have

$$\theta + \theta\gamma - 2\gamma\delta < \theta\gamma - \theta < 0 \text{ and } \theta + \theta\gamma - 2\gamma^2\delta > \theta - \theta\gamma > 0.$$

Hence $m'_1 + m'_2 = \frac{2}{a}(\theta - \gamma\delta)(\theta + \theta\gamma - 2\gamma\delta) > 0$, $m_1 + m_2 = -2\frac{\theta - \gamma\delta}{\gamma a}(\theta + \theta\gamma - 2\gamma^2\delta) < 0$, and the conclusion follows. The bifurcation diagram is depicted in Figure 8 (VII). When $l_1(0) < 0$, a limit cycle arises for $\mu_2 > \frac{\theta - \delta}{\theta(\gamma - 1)}\mu_1$.

If the slope of H is denoted by $m_H = \frac{\theta - \delta}{\theta(\gamma - 1)}$ and $m_{C_1} = e_1$, $m_{C_2} = e_2$, $m_{T_1} = \frac{\delta}{\theta}$ and $m_{T_2} = \frac{1}{\gamma}$ represent the slope of the straight line C_1 , C_2 , T_1 , T_2 , respectively, then (28) leads to the following order for the slopes of the curves:

$$m_{T_1} < m_{C_1} < m_H < m_{C_2} < m_{T_2} < 0.$$

Case 2. In the following we consider $\theta - \gamma\delta > 0$. Hence, from (19), we have $\lambda_1\lambda_2 < 0$. Therefore the equilibrium point E_3 is a saddle, provided that it exists.

Case 2.a) Consider $\theta - \gamma\delta > 0$, $\delta > 0$, and $\theta < 0$. Then $p > 0$ and there are no Hopf bifurcation. But we have $\Delta > 0$, $a > 0$. The equilibrium point E_3 exists if and only if $\delta\mu_1 - \theta\mu_2 > 0$ and $\mu_1 - \gamma\mu_2 > 0$. The bifurcation diagram is depicted in Figure 8 (VIII).

Case 2.b) Consider $\theta - \gamma\delta > 0$, $\delta > 0$, and $\theta > 0$. Then $\gamma\delta < 0 < \theta$ and $\Delta > 0$. The bifurcation diagram is depicted in Figure 9 (IX).

Case 2.c) Consider $\theta - \gamma\delta > 0$ and $\delta < 0$. Then $\theta > \gamma\delta > 0$, which leads to $\Delta < 0$ and $a > 0$. The bifurcation diagram is depicted in Figure 9 (X).

In conclusion, we have obtained *twelve bifurcation diagrams* corresponding to all possible situations. The Hopf bifurcation and, consequently, the existence of limit cycles emerging from the bifurcation are only possible in the bifurcation diagram VII (Figure 8), corresponding to the Case 1.c). All possible types of the four equilibrium points arising in the diagrams are summarized in Table 1 and Table 2. There are *twenty six* distinct generic phase portraits appearing in the bifurcation diagrams.

	1	2	3	4	5	6	7	8	9	10	11	12	13
O	s	un	s	s	sn	s	sn	sn	s	s	un	s	s
E_1	un	-	-	-	s	s	s	un	-	-	s	s	s
E_2	-	-	un	s	s	-	s	s	s	-	-	un	s
E_3	-	-	-	un	un	un	uf	-	uf	-	-	-	un

Table 1: *The types of the equilibrium points of system (4) on different regions of the bifurcation diagrams; the abbreviations s, sn, un, sf, and uf stand for saddle, stable node, unstable node, stable focus, and unstable focus, respectively.*

	14	15	16	17	18	19	20	21	22	23	24	25	26
O	s	s	s	s	sn	s	s	un	s	s	sn	un	s
E_1	s	s	s	sn	-	s	un	-	-	-	s	sn	sn
E_2	s	s	s	s	s	-	-	-	un	s	s	-	un
E_3	uf	sf	sn	-	-	-	s	s	s	-	-	s	s

Table 2: *Continuation of Table 1.*

4 Conclusions

A conclusion can be drawn from Theorems 2.12-2.13 and the above twelve bifurcation diagrams. It is given in the next theorem. Its proof is a direct consequence of the fact that, in all the above results from this section (with the exception of the case when a Hopf bifurcation occurs), we only needed terms up to order two in (4). These include also the case $a = 0$ because the curves $C_{3,4}$ do not change qualitatively the behavior of the system (the node-focus topological equivalence).

Theorem 4.1. *Assume $\theta\delta \neq 0$ and $\theta - \gamma\delta \neq 0$. If $\theta < 0$ or $0 < \gamma\delta < \theta$ or $\gamma\delta < 0 < \theta$, the system (4) is locally topologically equivalent near the origin to*

$$\begin{cases} \frac{d\xi_1}{dt} &= \xi_1 (\mu_1 - \theta\xi_1 + \gamma\xi_2) \\ \frac{d\xi_2}{dt} &= \xi_2 (\mu_2 - \delta\xi_1 + \xi_2) \end{cases} .$$

5 Acknowledgments

This research was supported by Horizon2020-2017-RISE-777911 project. We thank to Prof. Jaume Llibre for his useful suggestions in elaborating the article and to the anonymous referee for his valuable comments.

References

- [1] D. Adak, N. Bairagi and R. Hakl, Chaos in delay-induced Leslie-Gower prey-predator-parasite model and its control through prey harvesting. *Nonlinear Analysis: Real World Applications* 51 (2020), 1–19.
- [2] J. Belmonte-Beitia, Existence of travelling wave solutions for a Fisher-Kolmogorov system with biomedical applications. *Communications in Nonlinear Science and Numerical Simulation* 36 (2016), 14–20.
- [3] F. Brauer and C. Castillo-Chavez, *Mathematical Models in Population Biology and Epidemiology*, Springer-Verlag, Heidelberg, 2000.
- [4] M. Bulicek and J. Malek, Large data analysis for Kolmogorov's two-equation model of turbulence. *Nonlinear Analysis: Real World Applications* 50 (2019), 104–143.
- [5] H. I. Freedman, *Deterministic Mathematical Models in Population Biology*, Marcel Dekker, New York, 1980.
- [6] M. Kot, *Elements of Mathematical Ecology*, Cambridge University Press, 2001.
- [7] G. Laval and R. Pellat, Plasma physics, in: *Proceedings of Summer School of Theoretical Physics*, Gordon and Breach, New York, 1975.
- [8] J. Llibre and T. Salhi, On the dynamics of a class of Kolmogorov systems. *Applied Mathematics and Computation* 225 (2013), 242–245.
- [9] R. M. May, *Stability and Complexity in Model Ecosystems*, Princeton, New Jersey, 1974.

- [10] L. Perko, *Differential Equations and Dynamical Systems*, Third Edition, Springer–Verlag, New York, 2001.
- [11] M. Rafikov, J. M. Balthazar and H. F.von Bremen, Mathematical modeling and control of population systems: Applications in biological pest control. *Applied Mathematics and Computation* 200(2) (2008), 557–573.
- [12] Y. Yang, C. Wu and Z. Li, Forced waves and their asymptotics in a Lotka–Volterra cooperative model under climate change. *Applied Mathematics and Computation* 353 (2019), 254–264.